Thermochimica Acta, 143 (1989) 221–237
Elsevier Science Publishers B.V., Amsterdam – Printed in The Netherlands

THERMOGRAVIMETRIC IDENTIFICATION AND ANALYSIS OF REACTION PRODUCTS DURING OXIDATION OF SOLID OR LIQUID SULFIDES

F. AJERSCH and M. BENLYAMANI

Ecole Polytechnique, Campus de l'Université de Montreal, Montréal, Québec H3C 3A7 (Canada)

(Received 9 August 1988)

ABSTRACT

The reaction of metal sulfides in oxidizing atmospheres is an important stage in the extraction of copper, lead and zinc. Sulfide concentrates are usually roasted in air to the desired degree of oxidation and then treated further in a hydrometallurgical or pyrometallurgical process. An experimental method was developed in which the oxidation rates are controlled by the diffusion of reaction gas to the sample surface. The rate of weight change is related to the flux of reaction and product gas, including condensed reaction products, by means of an analytical formulation for each specific reaction stoichiometry. The method can be used to determine the exact reaction sequence during oxidation and the phase relationships that occur during the reaction process.

INTRODUCTION

The extraction of copper, zinc or lead in pyrometallurgical operations normally requires a roasting procedure to eliminate sulfur and to transform the product either as a sulfate or as an oxide. This process can take place in a fluid bed or in a multiple-hearth roaster for solid concentrates. For liquid sulfides, air or oxygen-enriched air is normally injected into a convector vessel.

An experimental technique using a microbalance has been used successfully in the determination of the various reaction sequences that take place during the elimination of sulfur, for both liquid sulfides [1–3], and solid [4] particulate sulfide materials. The method uses the continuous rate of weight change of a reactant placed in a crucible or sample tube of specific geometry, where the reaction is always controlled by the rate of diffusion of the reaction gas to the sample surface. By knowing the value of the interdiffusion coefficients of the reaction and product gases, and assuming that the rate of the chemical reaction is essentially instantaneous, an analytical expression for the calculation of the flux of reaction gas for a specific reaction can be formulated. Conversely, if the weight change of the

0040-6031/89/$03.50

reaction is determined accurately by the microbalance, the technique can also be used to determine the values of the gas interdiffusion coefficients.

This method of analysis was applied to the results of the oxidation of liquid Cu_2S, Cu, and FeS as well as for solid particulate samples of ZnS, FeS, (Zn,Fe)S and PbS.

EXPERIMENTAL

The experimental technique used in this study is an adaptation of a classical thermogravimetric method for the determination of gas interdiffusion coefficients of the vapors of organic materials of variable volatility [5,6]. The sample tubes used for the oxidation of liquid Cu and Cu_2S were made of quartz or VYCOR; alumina tubes were used for the oxidation of liquid FeS [2] and MgO tubes were used for the oxidation of all the particulate sulfide samples [4].

The effect of tube length and tube diameter has been established in a previous study [1] for sample tubes of 2–7 cm in length and 0.40 cm in diameter and for variable reaction gas flow rates from 20 to 400 ml min^{-1}. An optimum length of 5 cm was chosen for these experiments with internal diameters of about 0.5 cm.

Concentrations of reaction gases above 50% oxygen caused the reaction at liquid surfaces to proceed too rapidly and, consequently, experiments on the liquid and solid sulfides were carried out with gas mixtures containing less than 21% O_2.

No chemical analysis was made of the reaction products of the oxidation of liquid materials, but the particulate solid sulfide products were identified using X-ray diffraction at different stages of the reaction.

ANALYSIS OF THE REACTION KINETICS

When a reactive gas is passed over the surface of an open tube containing the sulfide sample, concentration gradients will be established in the gases within the tube. In order to fix these boundary conditions, the geometry of the tube needs to be specified such that the concentration of the gases at each extremity is kept constant, and that the flux of reaction and product gas is controlled by gas diffusion as shown in Fig. 1. If this geometry remains fixed throughout the reaction period, a steady-state rate of weight change is observed for each specific reaction. When the reaction mechanism changes, a new rate is observed.

Since the concentration of the liquid reactants is essentially constant at the interface, a steady-state weight loss is observed until a new reaction takes place. When solid reaction products appear on the liquid surface, the

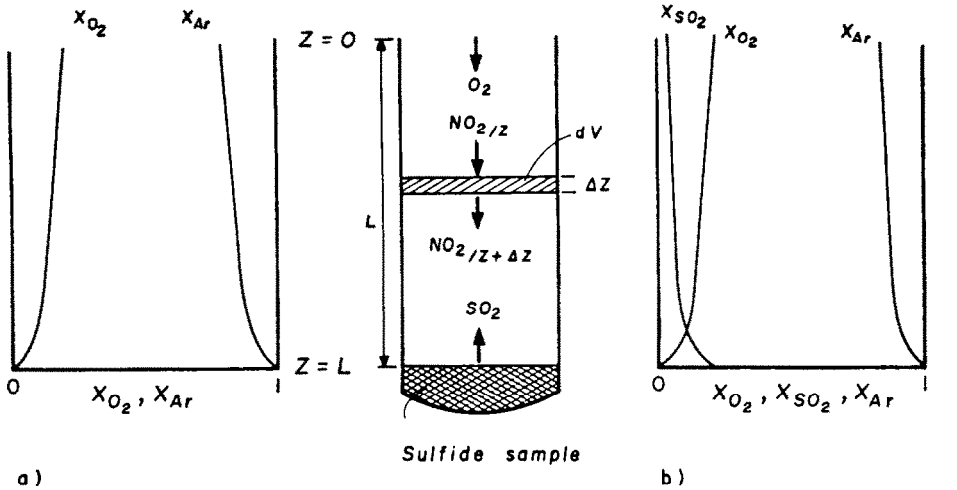

Fig. 1. Scheme to show the crucible and boundary conditions for (a) absorption of O_2 only and (b) reaction of sulfide with oxygen to form SO_2.

rates become non-linear because the formation of a solid product implies a reaction controlled by a solid-state diffusion mechanism. This is particularly evident in the case of the roasting of solid particulate sulfides where only the initial reaction can be considered to be gas-diffusion controlled.

From thermodynamic calculations it can be shown that the product reaction gas at this temperature is predominantly SO_2. A general expression for the sulfide reaction can be written as

$$\underset{\text{(solid)}}{\text{MS}} + k\underset{\text{(gas)}}{O_2} \rightarrow \underset{\text{(solid)}}{\text{Product}} + \underset{\text{(gas)}}{SO_2} \tag{1}$$

where MS represents the metal sulfide reactant and the solid product is either an oxide, an oxysulfide, or a sulfate. The ratio of the molar fluxes of the reaction and product gases is then given by

$$N_{SO_2} = -\frac{1}{k} N_{O_2} \tag{2}$$

where k is the stoichiometric factor. If argon is used as a diluent gas, the net flux of argon is zero, i.e. $N_{Ar} = 0$.

The Stefan–Maxwell equation for determining the fluxes of the three components SO_2, O_2 and Ar is

$$\frac{dX_i}{dz} = \sum_{j=1}^{3} \frac{1}{cD_{i-j}} \left(X_i N_j - X_j N_i \right) \tag{3}$$

and the gradient of oxygen in the zone above the reaction surface is given by

$$\frac{dX_{O_2}}{dZ} = \frac{1}{cD_{O_2-Ar}} \left(X_{O_2} N_{SO_2} - X_{SO_2} N_{O_2} \right) + \frac{1}{cD_{SO_2-O_2}} \left(X_{O_2} N_{Ar} - X_{Ar} N_{O_2} \right) \tag{4}$$

which can be solved [7] between the boundary conditions $Z = L$ and $Z = 0$, to give

$$X_{O_2} = \left[(X_{O_2})_0 - \frac{1}{1-(1/k)} - \frac{(X_{Ar})_0}{1-(1/k)(1-r_1)/(r_2-r_1)} \right] \times \exp\left[\left(1 - \frac{1}{k}\right) r_1 B N_{O_2} y \right] + \frac{1}{1-(1/k)} - \frac{(X_{Ar})_0 \exp(RBN_{O_2} y)}{1-(1/k)(1-r_1)/(r_2-r_1)} \tag{5}$$

with

$$X_{SO_2} + X_{O_2} + X_{Ar} = 1$$

and

$$B = \frac{L}{cD_{SO_2-Ar}} \qquad R = \frac{D_{SO_2-Ar}}{D_{O_2-Ar}} - \frac{1}{k}$$

$$r_1 = \frac{D_{SO_2-Ar}}{D_{SO_2-O_2}} \qquad r_2 = \frac{D_{SO_2-Ar}}{D_{O_2-Ar}} \qquad y = Z/L$$

The value of the molar flux of oxygen (N_{O_2}) can be solved using the Newton–Raphson method [8] by assuming that the concentration of oxygen at the gas–solid interface, $(X_{O_2})_0$, is negligible due to an instantaneous reaction. The gas interdiffusion coefficients, $D_{SO_2-O_2}$ and D_{SO_2-Ar} were calculated using the data of Chen and Othmer [9].

Since the value of the coefficient k is determined by the specific stoichiometry of the reaction, the flux of oxygen for a given length Z, can be determined analytically. This calculated value for specific values of k is compared to the value of the flux determined experimentally by taking the slope at $t = 0$ and which is given by

$$\frac{dm}{dt} = A(N_{O_2} M_{O_2} + N_{SO_2} M_{SO_2}) \tag{6}$$

where the rate of weight change of the sample of cross-section A is related to the absorption of oxygen to form a condensed phase, combined with the reaction of oxygen to produce SO_2 as represented by eqn. (6).

For the case of absorption or evaporation of a gas in a binary gas mixture such as oxygen–argon, the Stefan–Maxwell equation simply reduces to

$$N_{O_2} = -cD_{O_2-Ar} \frac{dX_{O_2}}{dz} + X_{O_2}(N_{O_2}) \tag{7}$$

which can be used to calculate the diffusion coefficient D_{O_2-Ar} when the flux of N_{O_2} is measured experimentally, so that

$$D_{O_2-Ar} = -\frac{(N_{O_2})(L)(X_{Ar})_{ln}}{c[(X_{O_2})_0 - (X_{O_2})_L]}$$

and

$$(X_{Ar})_{ln} = \frac{(X_{Ar})_L - (X_{Ar})_0}{\ln[(X_{Ar})_L/(X_{Ar})_0]}$$

RESULTS AND DISCUSSION

Oxidation at a gas–liquid surface

Liquid Cu and Cu_2S

A typical result of the oxidation of liquid Cu_2S is shown in Fig. 2. The decrease in weight is represented by the reaction

$$Cu_2S + O_2 \rightarrow 2Cu + SO_2 \quad (8)$$

or more simply by a reaction of the sulfur in the solution

$$\underline{S} + O_2 \rightarrow SO_2 \quad (9)$$

The oxidation stages may be illustrated by use of the adjacent Cu–S and Cu–O binary-phase diagrams shown in Fig. 3. The single-phase Cu_2S loses

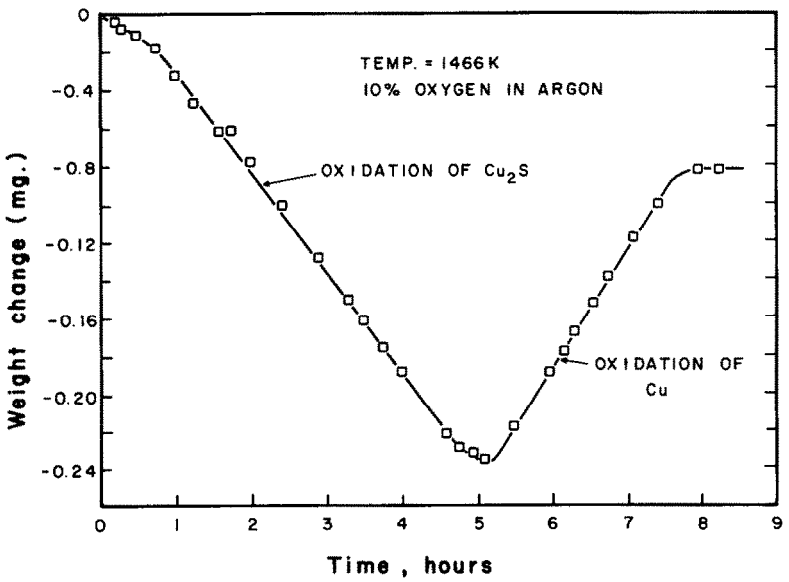

Fig. 2. Weight change for the oxidation of liquid Cu_2S at 1466 K with 10% O_2 in the reaction gas.

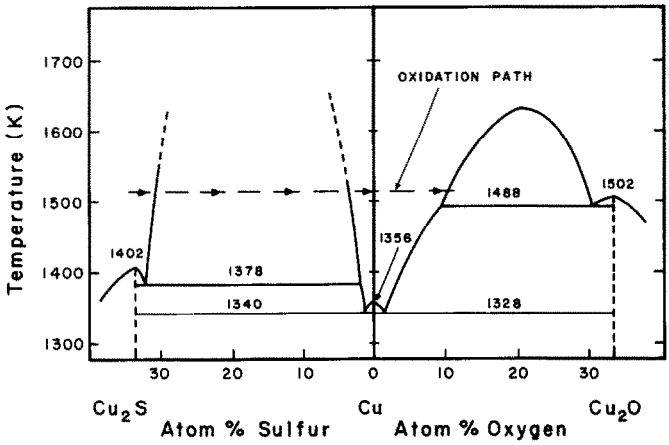

Fig. 3. Cu_2S–Cu–Cu_2O equilibrium diagram showing the oxidation path.

sulfur as SO_2. As the composition of the melt reaches the miscibility gap, the sample loses weight at a constant rate and continues at this rate until the sulfide phase disappears. The composition of both liquid phases in the region of the miscibility gap remains constant. Since the liquid copper produced by the reaction has a higher specific gravity than the liquid sulfide, it is expected that the settling of these small copper droplets will stir the sulfide phase, ensuring equilibrium at all times. This continuous mixing will prevent concentration gradients being established in both liquid phases.

After elimination of the copper sulfide phase, the sample continues to decrease in weight. In this region of low sulfur and low oxygen content, the rate slows down until a minimum weight is reached, when the rate of sulfur loss equals the rate of oxygen gain. Further oxidation then causes an increase in weight. The rate of weight change becomes linear over the range where the two phases, copper and copper oxide, are in equilibrium.

The effect of temperature on the reaction rate of liquid copper clearly indicated a transition from gas-diffusion control to solid-diffusion control when the melt starts to solidify (see Fig. 4).

Diffusion coefficients for the O_2–Ar gas mixture were calculated from the experimentally determined oxygen flux according to eqn. (7) and the results compare very well with those calculated from the empirical calculations of Chapman and Cowling [10] and of Chen and Othmer [9]. The experimental values and the calculated lines are shown in Fig. 5.

Liquid FeS

Similar experiments were carried out for the oxidation of liquid FeS [2] and this system proved to be more complex in nature. Samples of different sulfur contents (24.99% S and 31.00% S) in "FeS" were oxidized in the liquid state. The weight change results are shown in Fig. 6 and indicate that

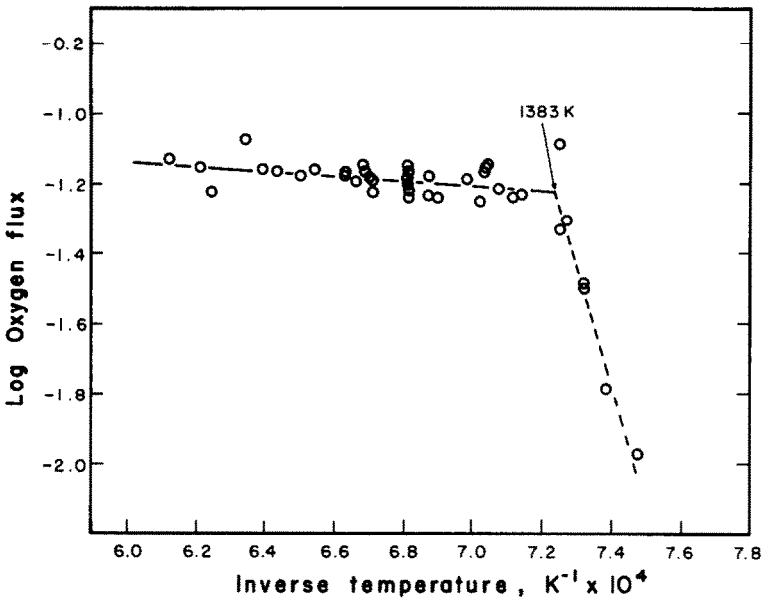

Fig. 4. Experimental values of the oxygen flux for the oxidation of Cu_2S.

the reaction proceeds in three distinct stages: (i) an initial weight increase; (ii) a weight decrease reaching a minimum value; and (iii) a final constant weight after complete reaction.

It was demonstrated that the solution of Fe + S was first oxidized by absorbing a limited amount of oxygen before the sulfur was oxidized. A

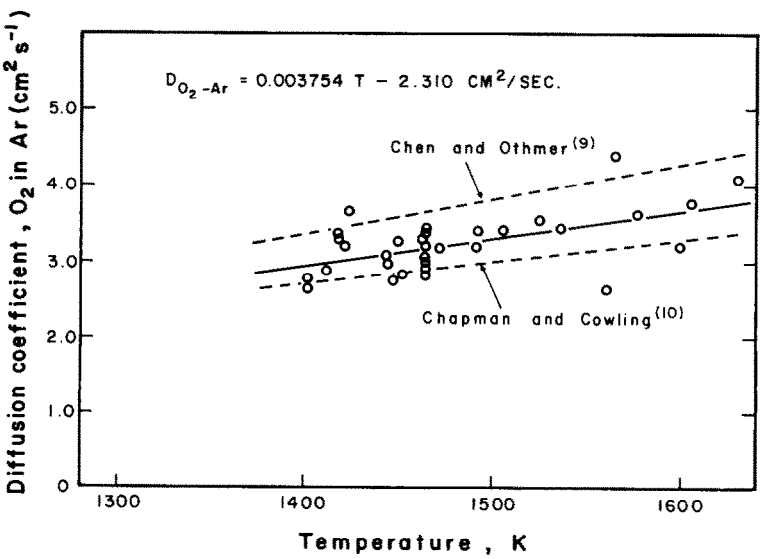

Fig. 5. Experimental values of the O_2–Ar diffusion coefficient as a function of temperature.

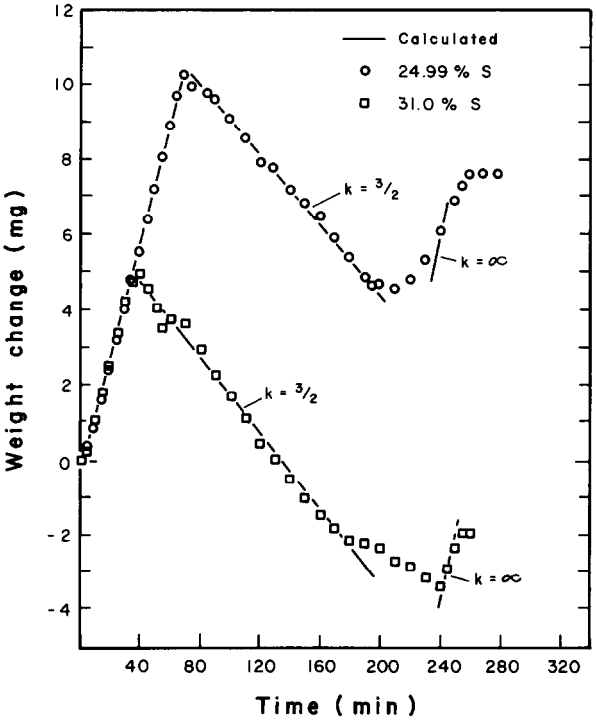

Fig. 6. Weight change for the oxidation of liquid FeS at 1473 K with 10% O_2 in the reaction gas for initial sulfur contents of 24.99% and 31.0%.

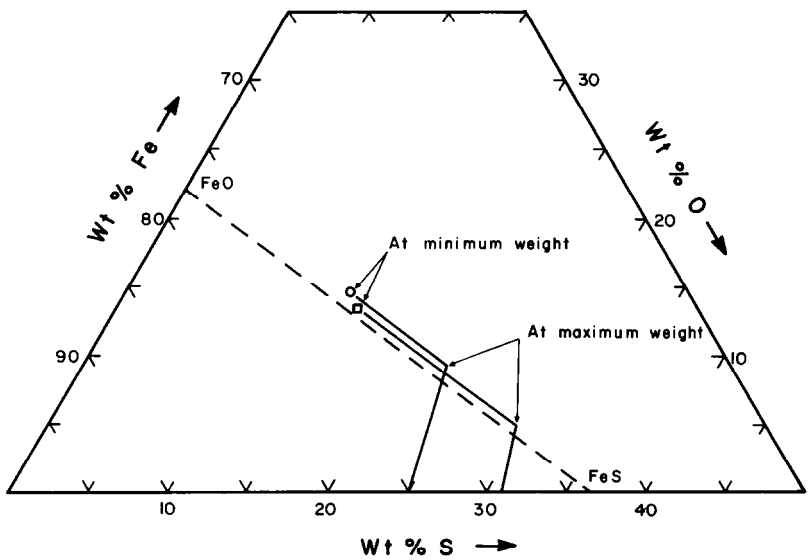

Fig. 7. The path of liquid FeS oxidation for samples of 24.99% S and 31.0% S.

ternary solution of $Fe + \underline{S} + \underline{O}$ is formed only when the activity of Fe is reduced. During this period, a steady-state weight increase is observed up to a maximum value which corresponds to a composition along the FeS–FeO quasi-binary diagram as shown in Fig. 7. Therefore sulfur is oxidized only in the second stage of the reaction which corresponds to a weight decrease.

The calculated values of weight change are shown as solid lines in Fig. 6 and clearly indicate that the stoichiometric coefficient corresponds to 3/2, representative of the reaction

$$FeS + \tfrac{3}{2}O_2 \rightarrow FeO + SO_2 \qquad (10)$$

The composition of the melt at the minimum weight was calculated from the amounts of SO_2 and O_2 exchanged at the melt interface and are indicated in Fig. 7.

The third reaction stage is again a weight increase and was shown to be due to the formation of magnetite in the melt. The magnetite activity was calculated and found to increase rapidly to 1.0 as the FeO content of the melt increased from 20 to 60 mol% [2]. Even though the final weight increase is not as clearly discernible as the previous reaction rates, it is still reasonably well represented by a rate which is controlled by the diffusion of oxygen to the reaction surface.

The experiments, therefore, clearly show that control of the reaction rate by gaseous diffusion distinguishes the sequence of reactions that occur when gaseous oxygen comes into contact with a liquid FeS melt.

Oxidation at gas–solid interfaces

When solid particulate sulfide material is placed into a sample tube and reacted in the same way as the liquid sulfide, the same mathematical analysis can be applied at the initial stages of reaction. This initial rate of weight change is not maintained due to the formation of a layer of solid reaction product on the particle surface by a mechanism of solid-state diffusion. In addition, sintering phenomena accompanied by agglomeration of the particles also cause the reaction to slow down because of the reduced area of reaction surface.

The limiting rate determined at $t = 0$ however, can be measured and compared to the calculated rates for a specific reaction using the same formalism that was used for the liquid sulfides, given by eqn. (6).

Solid ZnS

Figure 8 shows the weight change curves for the oxidation of pure ZnS with a 21% O_2 in argon mixture. It can be seen that the initial rates are nearly identical except for the slight differences which can be attributed to the change in the gas-interdiffusion coefficients with temperature.

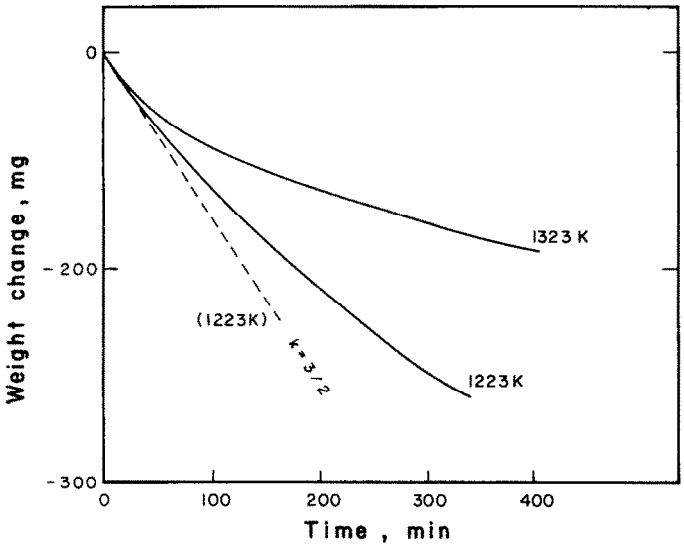

Fig. 8. Weight change for the oxidation of solid ZnS at 1223 and 1323 K with a reaction gas of 21% oxygen in argon.

A general decrease in the reaction rate with time is observed, decreasing more slowly at higher temperatures due to increased sintering of the ZnS particles. For the experimental conditions of this oxidation process, only ZnO should be formed according to the reaction

$$ZnS + \tfrac{3}{2}O_2 \rightarrow ZnO + SO_2 \qquad (11)$$

The dotted lines in Fig. 8 represent the rate of weight change that would be observed for a stoichiometric coefficient of 3/2 calculated using eqn. 6, and matches the experimental rate of weight change for the initial conditions ($t = 0$) as shown in Table 1. X-ray diffraction analysis of the reaction product indicated a pattern for ZnO only, as shown in Table 2.

Solid FeS

The reaction of solid FeS shows a weight change that resembles the oxidation of liquid FeS, which is shown by Fig. 9. Initially, no SO_2 gas is evolved during the reaction, as was also observed for the liquid FeS, indicating that only absorption of oxygen occurs during this stage. As the Fe–S–O solid solution becomes saturated in oxygen, a second reaction takes place generating SO_2 gas which was detected by passing the product gases through the LECO sulfur analyser.

A certain degree of overlap between reactions must take place because of the particulate nature of the sample. During the first stage, the solid-state diffusion of ionic iron plays a key role. The reaction products analysed by X-ray diffraction are Fe_3O_4 and FeS for experiments which were interrupted at this stage by quenching in argon. As has been shown previously [4], the

TABLE 1

The experimental and calculated flux of oxygen using the analytical model

System	Temp. (K)	k (calc.)	N_{O_2} (calc.) (mol cm^{-2} s^{-1}) $\times 10^{-6}$	N_{O_2} (exp.) (mol cm^{-2} s^{-1}) $\times 10^{-6}$	Specific chemical reactions
Oxidation of ZnS	1123	1.3	2.63	2.40	$ZnS + \frac{3}{2}O_2 \rightarrow ZnO + SO_2$
Oxidation of FeS (weight gain)	1123	—	2.68	1.66	$FeS_{1+\alpha} + \frac{3x}{2}O_2 \rightarrow \frac{x}{3}Fe_3O_4 + Fe_{1-x}S_{1+\alpha}$
Oxidation of FeS (weight loss)	1123	7/4	2.57	2.51	$FeS + \frac{7}{4}O_2 \rightarrow \frac{1}{2}Fe_2O_3 + SO_2$
Oxidation of solid-state phase of (Zn,Fe)S (weight loss)	1123	1.58	2.60	2.42	$\langle\langle ZnS\rangle\rangle + \frac{3}{2}O_2 \rightarrow ZnO + SO_2$ $\langle\langle FeS\rangle\rangle + \frac{7}{4}O_2 \rightarrow \frac{1}{2}Fe_2O_3 + SO_2$
Oxidation of PbS (weight gain)	873	3	1.61	1.52	$2PbS + \frac{7}{2}O_2 \rightarrow PbSO_4 \cdot PbO + SO_2$ $(\frac{3}{2}PbS + \frac{5}{2}O_2 \rightarrow \frac{1}{2}PbSO_4 \cdot 2PbO + SO_2)$
	923	3.42	2.01	1.92	$2PbS + \frac{7}{2}O_2 \rightarrow PbSO_4 \cdot PbO + SO_2$ $(\frac{3}{2}PbS + \frac{5}{2}O_2 \rightarrow \frac{1}{2}PbSO_4 \cdot 2PbO + SO_2)$
	973	3.5	2.06	2.00	$2PbS + \frac{7}{2}O_2 \rightarrow PbSO_4 \cdot PbO + SO_2$

$\langle\langle ZnS\rangle\rangle$ and $\langle\langle FeS\rangle\rangle$ represent constituents in solid solution.

TABLE 2

Identification of the principal products by X-ray diffraction

System	Temperature (K)	Products identified
Oxidation of ZnS	1123	ZnO
	1223	
Oxidation of FeS	1123	Fe_3O_4 (weight gain)
		Fe_2O_3 (final oxidation product)
Oxidation of (Zn,Fe)S	1123	ZnO, ZnF_2O_4
	1223	
Oxidation of PbS	873	PbS_4, $PbSO_4 \cdot PbO$
	923	$PbSO_4 \cdot PbO$, $PbSO_4$
	973	$PbSO_4 \cdot PbO$, $(PbSO_4)$*, $(PbSO_4 \cdot 4PbO)$
	1073	$PbSO_4 \cdot PbO$, $PbSO_4 \cdot 4PbO$

* Trace amount

production of Fe_3O_4 can proceed without loss of sulfur due to the stability of the two phases in the stoichiometry range of FeS from $Fe_{0.92}S$ to $Fe_{1.14}S$. The variation in the iron content arises from the migration of iron vacancies in the FeS and proceeds to oxidize the Fe^{2+} ions which diffuse to the surface and transform to Fe_3O_4 according to the reaction

$$FeS_{1+\alpha} + \tfrac{3}{2}xO_2 \rightarrow \frac{x}{3}Fe_3O_4 + Fe_{1-x}S_{1+\alpha} \tag{12}$$

where α is the excess fraction of sulfur atoms with respect to the stoichio-

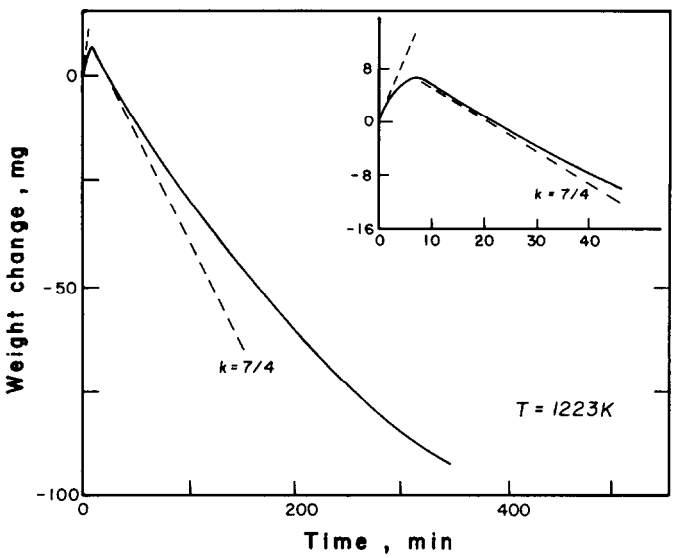

Fig. 9. Weight change for the oxidation of solid FeS at 1223 K with a reaction gas of 21% oxygen in argon.

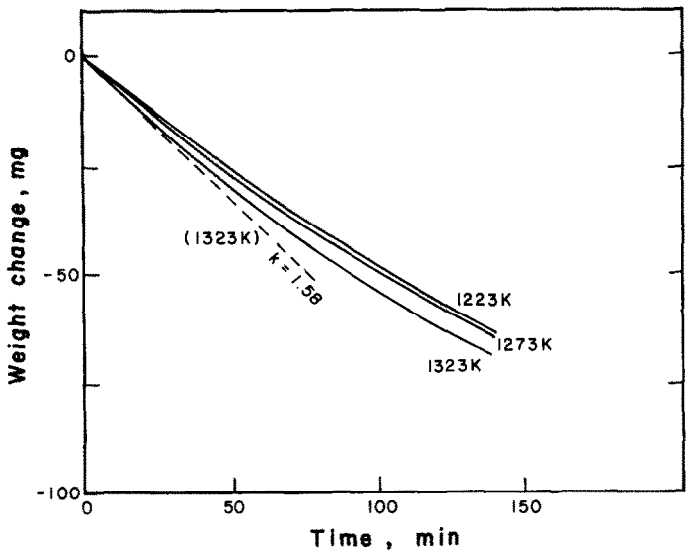

Fig. 10. Weight change for the oxidation of solid solution (Zn,Fe)S at 1223, 1273 and 1323 K with a reaction gas of 21% oxygen in argon.

metric value, and x is the fraction of iron atoms. This phenomenon was also observed by Niwa et al. [11] for the oxidation of FeS between 773 K and 973 K. These results show that the elementary reaction steps at a solid surface are the same for particulate as well as for bulk solid samples of FeS, and that this initial period of oxidation in the solid state is limited by the diffusion of iron.

Following the small initial weight increase the sample weight reaches a maximum and then decreases abruptly. The measured and calculated rate of weight change corresponds to the reaction

$$\text{"FeS"} + \tfrac{7}{4}O_2 \rightarrow \tfrac{1}{2}Fe_2O_3 + SO_2 \qquad (13)$$

where "FeS" is represented, in fact, by the non-stoichiometric $Fe_{1-x}S_{1+\alpha}$.

Figure 9 also shows the rate of weight change for a stoichiometric coefficient of 7/4 calculated using eqn. (6), and shown in Table 1, which matches the reaction products analysed by X-ray diffraction and which would be predicted from thermodynamic considerations.

Solid (Zn,Fe)S

The weight change pattern of the oxidation of particles of a (Zn,Fe)S solid solution of 75 mol% ZnS is shown in Fig. 10. A much more linear relationship is observed for this system with little effect of temperature. The X-ray analysis of the products indicated ZnO and $ZnFe_2O_4$, as shown in Table 2. The formation of the zinc ferrite ($ZnFe_2O_4$) is highly favored at this

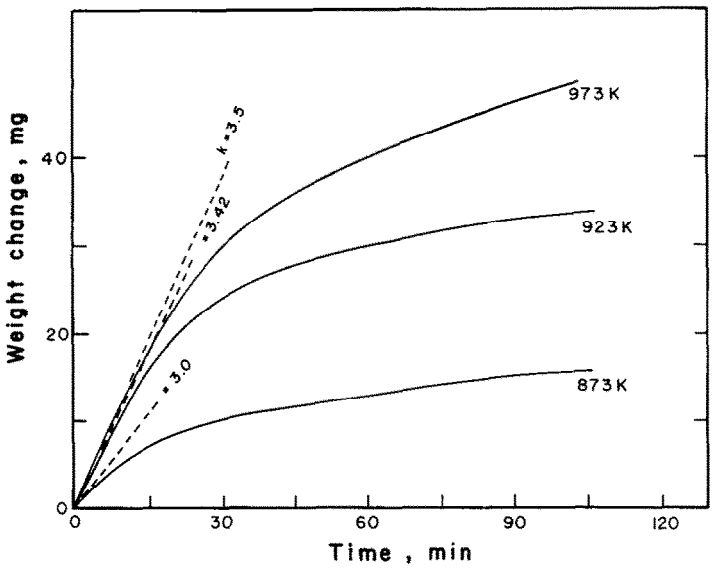

Fig. 11. Weight change for the oxidation of solid PbS at 873, 923 and 973 K with reaction gas of 21% oxygen in argon.

temperature where all the product Fe_2O_3 reacts instantaneously with the ZnO according to the reaction

$$ZnO + Fe_2O_3 \rightarrow ZnFe_2O_4 \tag{14}$$

The initial limiting rate of weight change for this reaction gave a stoichiometric coefficient of 1.58 as shown by the dotted line in Fig. 10 which is representative of the proportional amounts of ZnS ($k = 1.50$) and FeS ($k = 1.75$) in the solid solution.

Solid PbS

The evolution of the reaction products as a function of temperature can be determined from the weight change curves shown in Fig. 11 for the oxidation of PbS particles at 873, 923 and 973 K. A weight gain is observed due to the formation of $PbSO_4$ or other oxysulfates. As in the case of the other sulfides in particulate form, the initial rate of reaction decreases as the reaction proceeds. Figure 11 also shows the stoichiometric factor calculated for each reaction temperature as described previously for calculating the oxygen flux according to eqn. (6) and these values are indicated by the dotted lines in Fig. 11.

The possible reactions that occur can be given as follows

$$PbS + 2O_2 \rightarrow PbSO_4 \tag{15}$$

$$2PbS + \tfrac{7}{2}O_2 \rightarrow PbSO_4 \cdot PbO + SO_2 \tag{16}$$

$$\tfrac{3}{2}PbS + \tfrac{5}{2}O_2 \rightarrow PbSO_4 \cdot 2PbO + SO_2 \tag{17}$$

and

$$\tfrac{5}{4}PbS + 2O_2 \rightarrow \tfrac{1}{4}(PbSO_4 \cdot 4PbO) + SO_2 \quad (18)$$

where the stoichiometric factors k of the reaction and product gases are ∞, 3.5, 2.5 and 2, respectively. The experimental results indicate that the ratio of $PbO/PbSO_4$ increases with increasing temperature and tends towards a stoichiometric coefficient of 3.5, as shown in Table 1.

At 873 K, the agreement between the calculated and experimental values of the limiting slope ($t = 0$) is not very good because the chemical reaction rate at the gas–particle interface is slow enough to affect the overall reaction rate and thus gas diffusion is no longer the controlling factor. It should be noted that the oxidation temperature of PbS was considerably lower than for the other solid sulfides and, therefore, chemical kinetics will play a significant role.

APPLICABILITY OF THE MODEL

The results of the experiments of this study show that the mathematical analysis used in evaluating the stoichiometric reaction coefficients can be used to predict the most probable reaction that takes place, if the oxidation rate is controlled by gas diffusion.

For the case of oxidation of liquid Cu, Cu_2S and FeS, steady-state regions of weight change are obtained where the slope can be determined simply and accurately, thus verifying the exact reaction that takes place. When particulate materials are oxidized, this becomes less evident and a numerical method for calculating the initial reaction rate was developed as described previously, resulting essentially in an experimental value of the stoichiometric coefficient.

Table 1 summarizes the different chemical reactions for the oxidation of the particulate sulfides ZnS, FeS, (Zn,Fe)S, and PbS. The values of the stoichiometric coefficients and of the oxygen flux were calculated, and the latter were compared with the experimental values determined by eqn. (6) for each of the chemical reactions indicated. The results given in Table 1, therefore, are an indication of the applicability of the analytical model. The agreement for the oxidation of ZnS is excellent and clearly defines the reaction product as only ZnO and which was confirmed by X-ray diffraction as shown in Table 2.

The oxidation of particulate FeS shows a similar behavior to the oxidation of liquid FeS. During the weight-decrease stage, however, the reaction product was found to be Fe_2O_3 rather than FeO which can also be confirmed by thermodynamic predictions.

The oxidation of PbS at different temperatures shows a more complex evolution of reaction products. The analytical model results in the prediction of the formation of $PbSO_4 \cdot 2PbO$, but this phase was not detected by X-ray

diffraction analysis, as shown in Table 2. From thermodynamic considerations, Kellogg and Basu [12] have shown that this compound is unstable at temperatures below 889 K, and decomposes according to the reaction

$$3(PbSO_4 \cdot 2PbO) \rightarrow 2(PbSO_4 \cdot PbO) + PbSO_4 \cdot 4PbO \quad (20)$$

This reaction is very slow but can occur at temperatures below 723 K. Because the X-ray analysis of the reaction products is carried out at ambient temperature, it is not surprising that the bioxysulfate was not detected.

The mathematical analysis of the weight-change curves, however, clearly showed that the formation of $PbSO_4 \cdot 2PbO$ does in fact take place, as verified by the calculation of the stoichiometric coefficient, particularly at 923 and 973 K. This is most significant in that the experimental weight-change data resulted in the identification of the reaction products which were actually formed in situ, but which were not found by X-ray analysis of the reaction products because they were cooled down to ambient temperature for analysis. For example, the $PbSO_4$ phase was detected by X-ray diffraction for reactions at 873 and 923 K, but the analysis of the weight-change evolution does not indicate its formation. Decomposition reactions must obviously occur during the transition from reaction to ambient temperature.

At 973 K, $PbSO_4$ and $PbSO_4 \cdot 4PbO$ were detected only in traces and the predominant product was identified as $PbSO_4 \cdot PbO$, which is in excellent agreement with the calculated reaction product given by eqn. (6). This result is also in agreement with the results of Tuffley and Russel [13] who found that the monooxysulfate is the predominant reaction product for PbS oxidation in air between 873 and 1373 K.

CONCLUSION

An experimental technique has been developed for the oxidation of liquid or solid sulfide materials where the reaction rate is controlled by the inter-diffusion of the reaction gas to the reaction surface by fixing the physical and chemical boundary conditions of the reaction system. The method was used successfully in measuring the high-temperature diffusion coefficients of an oxygen–argon gas mixture for a known specific reaction (liquid Cu_2S), and also in identifying the reaction sequence of the oxidation of liquid FeS and solid particulate FeS, ZnS, (ZnFe), and PbS over a temperature range that is generally employed in the converting or roasting of these sulfide concentrates in conventional pyrometallurgical processes.

Analytical expressions were derived for the flux of the reaction gas for the specific reactions that can occur. When the experimental rate of weight change is compared to the calculated rate, the specific reaction can be identified by determining the corresponding stoichiometric coefficients.

X-ray diffraction analysis of the solid samples after reaction was used to verify the calculated reaction products, but did not always correspond to the products predicted from the mathematical analysis of the reaction system. This discrepancy was found to be due to the decomposition of reaction products when the temperature was reduced to ambient as has been observed in the case of the oxidation of PbS.

The mathematical analysis of the thermogravimetric data can, therefore, be used to identify the actual reaction sequence that occurs at the reaction temperature and can be applied to other gas–liquid or gas–solid reaction systems.

REFERENCES

1 F. Ajersch and J.M. Toguri, Met. Trans., 3 (1972) 2187–2193.
2 Z. Asaki, F. Ajersch and J.M. Toguri, Met. Trans., 5 (1974) 1753–1759.
3 Z. Asaki, S. Ando and Y. Kondo, Met. Trans. B, 19 (1988) 47–52.
4 M. Benlyamani and F. Ajersch, Met. Trans. B, 17 (1986) 647–656.
5 C.Y. Lee and C.R. Wilke, Ind. Eng. Chem., 46 (1954) 2381–2387.
6 J.F. Richardson, Chem. Eng. Sci., 10 (1959) 234–242.
7 M. Benlyamani, M.A.Sc. Thesis, École Polytechnique de Montréal, 1984.
8 B. Carnahan, H.A. Luther and J.D. Wilker, Applied Numerical Methods, Wiley, New York, 1969.
9 N.H. Chen and D.F. Othmer, J. Chem. Eng. Data, 7 (1962) 37–41.
10 S. Chapman and T.G. Cowling, The Mathematical Theory of Nonuniform Gases, Cambridge University Press, London, 1960, p. 237.
11 K. Niwa, T. Wada and Y. Shiraishi, Trans. AIME, 209 (1957) 296–301.
12 H.H. Kellogg and S.K. Basu, Trans. AIME, 218 (1960) 70–81.
13 J.R. Tuffley and B. Russel, Trans. AIME, 230 (1964) 950–956.